

The influence of sputtering on FeSi

H. C. SWART, G. L. P. BERNING

Department of Physics, University of the Orange Free State, P.O. Box 339, ZA-9300 Bloemfontein, Republic of South Africa

The effect of different (0.5, 2 and 4 keV) Ar⁺ energy ions on (a) the composition of an FeSi surface, (b) the oxidation of the FeSi surface after bombardment, and (c) the segregation of silicon after bombardment, has been monitored by Auger electron spectroscopy. Silicon was found to be preferentially sputtered by the Ar⁺ ions at all the different energies during bombardment. This effect was more pronounced at the 0.5 keV ion energy bombardment. There was a slight increase in the oxidation rate from the higher to the lower Ar⁺ ion energy at which the sample was sputtered before oxidation. The rate of silicon diffusion to the surface at 593 K after the sample had been sputtered, was lower when the sample had been sputtered by 0.5 keV ions than by 2 keV ions.

1. Introduction

The oxidation of silicon and metal silicides is of special importance in the integrated circuit technology [1]. With surface-sensitive techniques such as Auger electron spectroscopy (AES) and X-ray photoelectron spectroscopy (XPS), the initial surface oxidation at room temperature and at oxygen pressures in the high-vacuum range can be measured. Such studies have been reported on various metal silicides [2–4]. In these studies it is unavoidable to clean the surface by sputtering before oxidation can be measured.

It is well known that for various silicides, sputtering with Ar⁺ ions resulted in a depletion of the silicon component on the surface as measured by AES [5]. During ion bombardment of a multicomponent sample, the surface composition changes initially as an altered layer develops. Eventually a steady state is reached when the altered layer becomes constant. This altered layer recedes into the target with time during sputtering [4]. Smith and Walls [6] discusses three qualitatively situations for elastic collisions of random materials which are categorized as the single knock-on regime, the linear cascade regime and the spike regime. When a surface is bombarded with low-energy ions, the knock-on regime dominates and the damage caused by the ions is more restricted to the surface layer. When bombarded with higher energy ions the other two regimes dominate and a much deeper altered layer with higher defect concentration is produced. The composition of the altered layer will thus depend on the energy of the bombarding ions. When the projectile energy is changed, the previously steady state acts as a bulk material for the sputtering and has to be sputtered away before the new steady state is obtained [4]. The surface composition immediately after a change in the sputtering energy depends on the composition of the altered layer created by the first ion energy and the change in surface composition during the build-up of the new altered layer at the second ion energy.

The monitoring of the high- and low-energy Auger peaks is a suitable method for detailed composition profiling. The high-energy peaks can be used to determine the near surface composition (escape depth between 1 and 2 nm), while the low-energy peaks provide information on the surface composition (escape depth of about 0.4–0.6 nm) [7].

In the present paper we report (a) the composition change of FeSi during sputtering with Ar⁺ ions of different energies and (b) the oxidation of FeSi (i) after sputtering at different ion energies, and (ii) after the sample was annealed at 593 K in order to increase the silicon content in the surface region. The concentration of silicon was determined from Auger peak-to-peak heights (APPH) and corrected for matrix influence.

2. Experimental procedure

A 150 nm iron layer was deposited onto a clean Si(100) substrate by electron-beam heating of pure iron in a vacuum system ($< 1 \times 10^{-6}$ torr; 1 torr = 133.322 Pa). The sample was then heated for 25 min at 823 K to produce a film of FeSi.

In the first experiment the FeSi sample was bombarded sequentially with Ar⁺ ions of 0.5, 2, and 4 keV at an argon pressure of 5×10^{-5} torr. The APPH of the 47 eV Fe, 92 eV Si and the 703 eV Fe peaks were monitored by a multiplexer during sputtering at the different ion energies. An Auger spectrum was recorded at each ion energy after the sample was sputtered, until equilibrium was attained. This procedure was repeated for pure silicon and for pure iron.

In the second experiment, the FeSi sample was oxidized after sputtering. The following procedure was followed for each of the oxidation studies. The sample was sputtered with 0.5 keV Ar⁺ ions at an argon pressure of 5×10^{-5} torr until equilibrium was attained. Then the system was pumped down to a base pressure of 1×10^{-9} torr before oxidation. During

oxidation the main valve to the pump was slightly opened and the oxygen was admitted into the system through a leak valve to maintain the required pressure (8×10^{-8} torr). A full range of Auger spectra (0–1000 eV, modulation 4 eV) and detail spectra (30–100 eV, modulation 0.5 eV) were recorded after various oxygen exposures. This procedure was repeated for Ar^+ ions with energies 2 and 4 keV. In order to minimize the effect of the electron and the ion gun, the beam voltage of the electron gun was switched on only when the spectra were recorded and the ion gun was switched off after sputtering. Extra care was taken to ensure that the conditions were the same for each oxidation.

In the third experiment, the FeSi sample was annealed at 593 K while being bombarded with 0.5 keV Ar^+ ions. After concentration equilibrium was reached the ion beam was switched off and the Si (92 eV) APPH was monitored until a new equilibrium was attained. The sample was then cooled down to room temperature and oxidized as previously discussed. This was repeated for 2 keV Ar^+ ion bombardment. The annealing temperature was chosen low enough to prevent the formation of FeSi_2 . (Our previous experiments indicated that FeSi_2 starts to grow at 800 K.)

The system used for the Auger analysis was an AES Physical Electronics Model 545 equipped with a double-pass cylindrical mirror analyser and a coaxial electron gun. The angle between the direction of the incident electron beam and the normal to the surface was 30° . An electron beam energy of 3 keV and a beam current of $20 \mu\text{A}$ were used for all the Auger analysis. The angle between the direction of the incident ion beam and the normal to the surface was 40° . The ion current densities were 38, 30 and $14 \mu\text{A cm}^{-2}$ for 4, 2, and 0.5 keV, respectively.

3. Results and discussion

3.1. Composition

The APPH for pure silicon and pure iron versus the sputtering time for the different primary Ar^+ ion energies (0.5, 2 and 4 keV) are shown in Fig. 1a. The changes in the low-energy APPH when the sample is sputtered sequentially with ions of different energies are due to changes in the slope of the low-energy secondary electrons in the $N(E)$ spectrum. The effect of the ion-beam energy on the APPH of silicon and iron in FeSi are shown in Fig. 1b. The low energy APPH of iron and silicon in Fig. 1a were used as standards in Briggs and Seah's formalism [8] with calculated backscattering factors [9] to calculate the concentration of silicon from Fig. 1b, and this is presented in Fig. 1c. It should be emphasized that the concentration values determined from the low-energy Auger peaks correspond to an electron escape depth of about 0.4–0.6 nm [10]. It is clear from Fig. 1c that when the bombarding energy is changed the surface composition changes rapidly followed by a transient period during which a new steady state is attained. For all the different sputtering energies, the silicon is preferentially sputtered. The fast drop in silicon, when

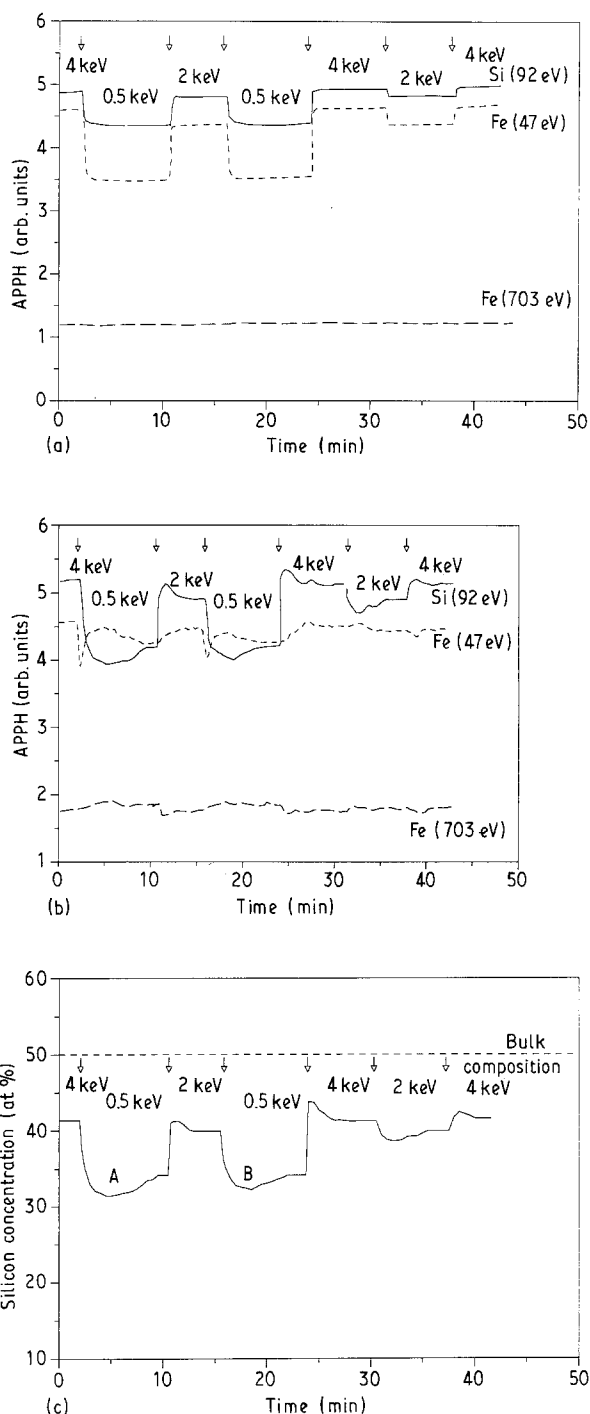


Figure 1 The APPH of silicon and iron for (a) pure silicon and pure iron, and (b) for FeSi, versus the sputtering time for Ar^+ ion energies of 0.5, 2 and 4 keV. The concentration variation on the FeSi surface during the different Ar^+ ion bombardment are shown in (c).

changing from the higher ion energies of 2 or 4 keV to the lower energy of 0.5 keV, indicates a higher preferential sputtering of silicon in the top layers of the sample for the lower energy ions.

By using the low-energy Ar^+ ions, which are more surface sensitive, after sputtering with higher energy Ar^+ ions, a depth profile of the previously altered layer can be obtained (bearing in mind the preferential sputtering of silicon). The silicon surface concentration for the two regions A and B in Fig. 1c are shown enlarged and as a function of depth in Fig. 2a. The minima for silicon indicate a depletion zone of silicon which developed beneath the surface during sputtering with higher energy ions. The existence of a

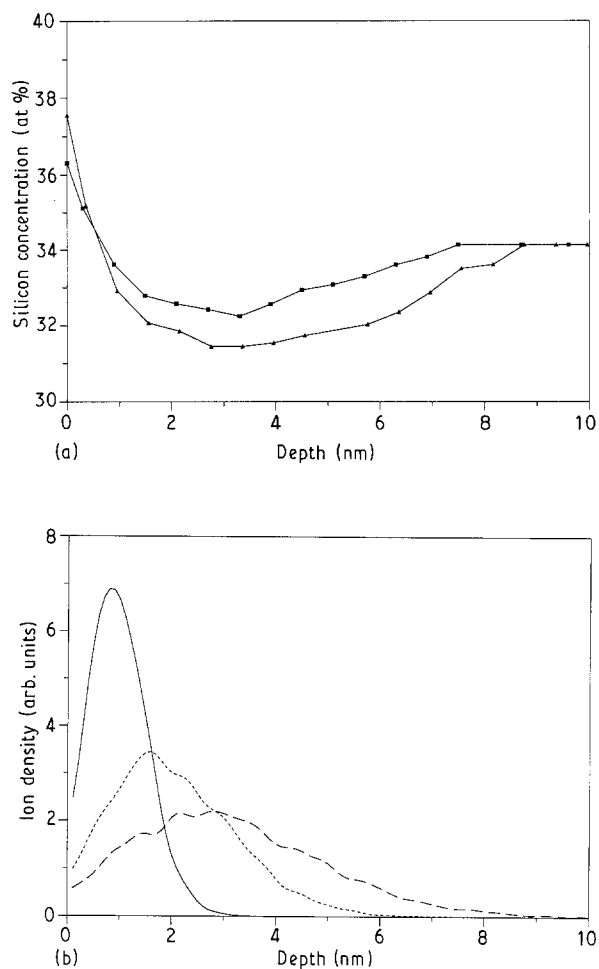


Figure 2 (a) The silicon surface concentration of FeSi while sputtering with an energy of 0.5 keV after sputtering with (■) 2 and (▲) 4 keV Ar⁺ ions. (b) The ion range distribution of the (—) 0.5, (---) 2 and (—) 4 keV Ar⁺ ions in FeSi, calculated with TRIM-88 [14] at an angle of 40°.

depletion region after sputtering a multicomponent system is commonly observed [11, 12]. As previously reported [13] this behaviour can be explained by surface segregation assisted by irradiation-enhanced diffusion. The silicon was slightly more depleted in this zone after sputtering at 4 keV than after sputtering at 2 keV and the transient region after bombardment with 4 keV ions was also a little broader than that after 2 keV ion bombardment. Calculations done with the Monte Carlo simulation program TRIM [14] developed by Biersack and Haggmark [15], are given in Fig. 2b, which shows the ion range distribution of the different energy Ar⁺ ions in FeSi calculated for an ion incident angle of 40°. This is the same angle as in the experiments. The 2 keV ion range varied between 0 and 6 nm while that of the 4 keV ions varied between 0 and 9 nm. By comparing these projected ion ranges with the sputtered altered layers, Fig. 2a, it is clear that the range of the ions determine the depth of the altered layers formed during sputtering. The sharp drops (at 0 nm) in Fig. 2b towards the surface are due to the leakage of ions through the surface.

Table I shows the surface and the near surface silicon concentrations at the different steady states during sputtering as a function of the ion energy. The low-energy 47 eV Fe and 92 eV Si peaks were used to

TABLE I The silicon equilibrium concentration, at the steady states conditions, for the different energy Ar⁺ ions

Ar ⁺ ion energy keV	Si concentration (at %)	
	Surface	Near surface
0.5	34	35
2	40	38
4	42	39

calculate the surface concentration (escape depth of about 0.4–0.6 nm) and the 703 eV Fe and 1619 eV Si peaks for the near surface concentration (escape depth between 1 and 2 nm) [7]. The silicon surface concentration increases with the energy of the Ar⁺ ions with a much lower concentration for 0.5 keV and is lower than the bulk value (50 at%) in all three cases. The near surface concentration was lower than the surface concentration for the 2 and 4 keV ion bombardment, indicating again that a depletion zone developed beneath the FeSi surface during sputtering with the higher energy ions.

3.2 Oxidation

Fig. 3a–c show the Auger profiles for FeSi exposed to oxygen after the surface was sputter clean at the indicated Ar⁺ ion energies. The low-energy iron and silicon peaks at 0 L (L = 1 × 10⁻⁶ torr.s) are very similar after sputtering at the different ion energies, except for the difference in the relative intensities of the peaks due to the different concentrations. The changes in the silicon peaks in Fig. 3a–c are due to the oxidation of silicon on the surface. The silicon peak shifts to 80 eV for silicon in SiO₂ [16]. The changes in the silicon peaks in Fig. 3b and c at similar exposures are almost the same, while the changes in the peaks in Fig. 3a suggest slightly more oxidation of silicon than in Fig 3b and c. During the oxidation of iron, the low-energy iron peak shifts from 47 eV to 44 and 52 eV [17]. Because there is no change in the position of the iron peaks, one can infer that the iron does not oxidize for oxygen exposures up to 1000 L. The oxygen concentration versus exposure plots in Fig. 4a–c, which corresponds to the spectra in Fig. 3a–c, give a better indication of the oxidation of the silicon as a function of exposure, showing a slight increase in oxidation from the higher to the lower Ar⁺ ion energy at which the sample was sputtered before oxidation. The Palmberg method [18] was used to determine the oxygen concentration.

3.3 Segregation

Fig. 5 shows the surface concentration of silicon against time for the FeSi sample at 593 K during and after bombardment at this temperature with 2 and 0.5 keV Ar⁺ ions. It is clear that the rate of silicon diffusion to the surface after the sputtering had been stopped (position G), is higher when the sample had been sputtered by 2 keV ions than by 0.5 keV ions. The higher energy ions will disturb the surface layer and create defects to a greater depth with a higher

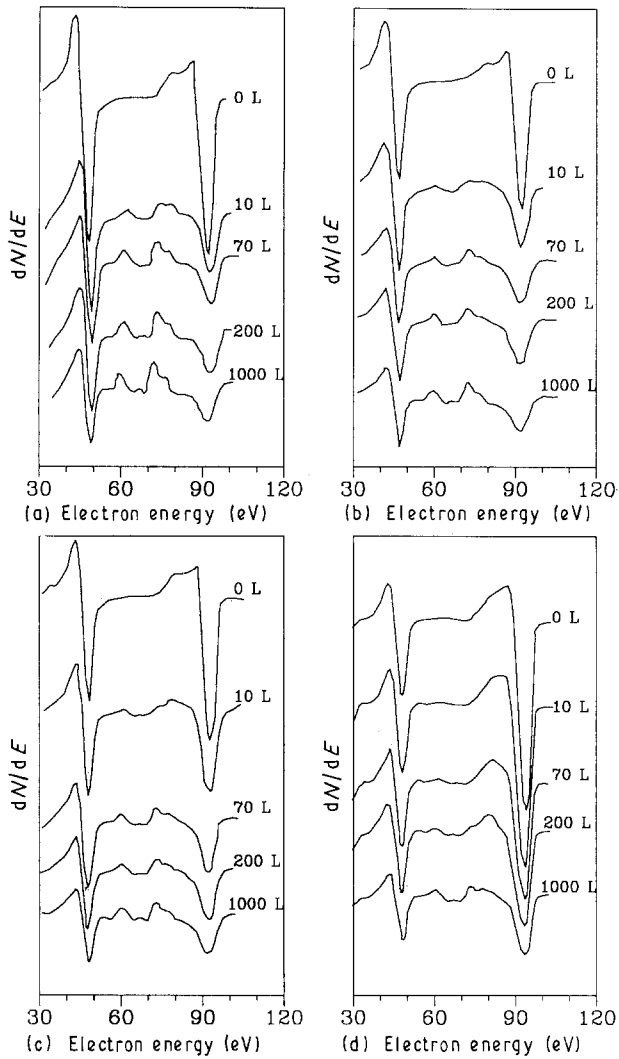


Figure 3 Low-energy Auger spectra of FeSi exposed to oxygen after the surface was sputtered clean at (a) 0.5, (b) 2 and (c) 4 keV Ar^+ ion energies. Spectra (d) were recorded at room temperature, during oxygen exposure, after the sample was sputtered and then annealed at 593 K until equilibrium was reached.

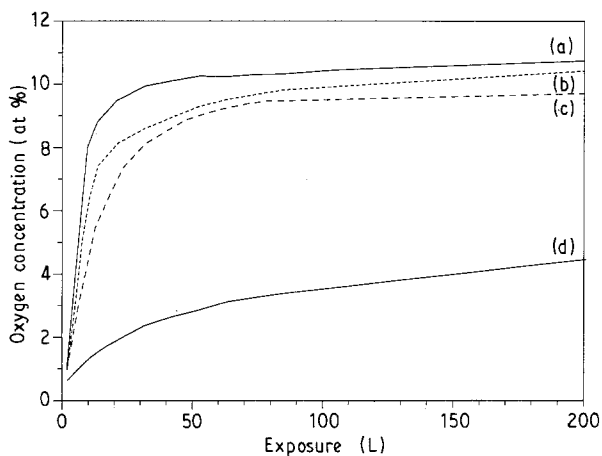


Figure 4 Oxygen uptake curves after the FeSi surface was sputtered clean at (a) 0.5, (b) 2, (c) 4 keV Ar^+ ion energies and (d) after the sample was sputtered and then annealed at 593 K until equilibrium was reached.

concentration than the 0.5 keV ions. The silicon diffusion in the disturbed surface with the higher defect concentration is higher than in the less disturbed surface with lower defect concentration caused by the

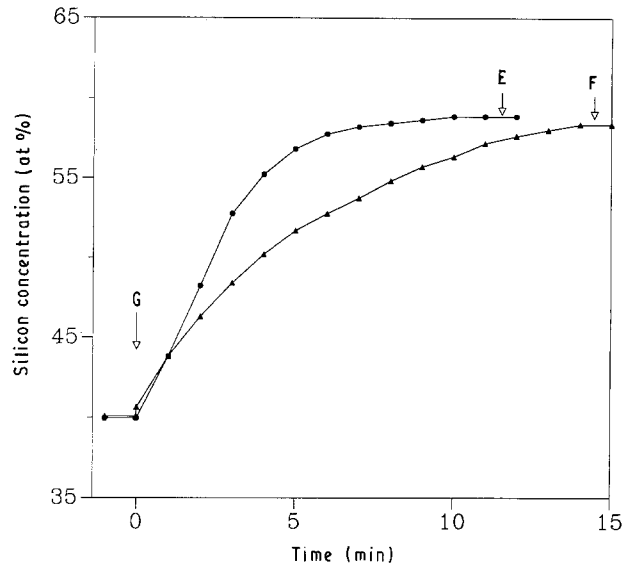


Figure 5 The silicon concentration versus time for the FeSi sample during and after bombardment with (●) 2 keV and (▲) 0.5 keV Ar^+ ions at 593 K. The sputtering was stopped at G.

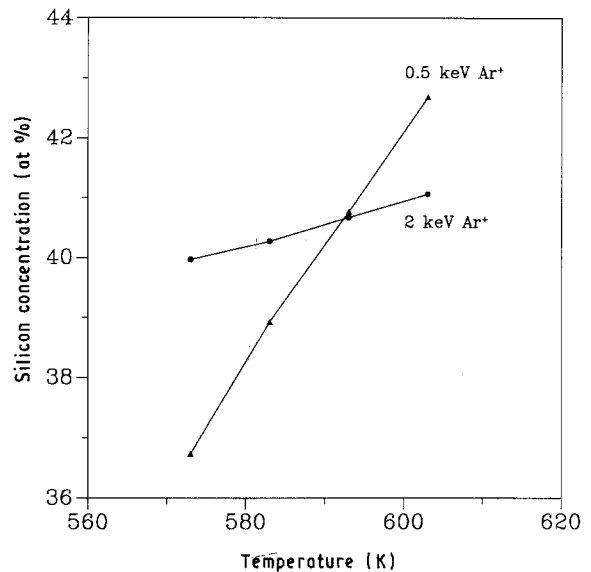


Figure 6 The silicon concentration versus temperature for the FeSi sample during sputtering with 2 keV and 0.5 keV Ar^+ ions.

0.5 keV ions. The silicon surface concentration after equilibrium was attained after sputtering was 58 at% (position E and F). The near surface concentration, for both cases, was 45 at%. Fig. 6 shows the change in the silicon surface concentration after equilibrium was reached during sputtering at different temperatures with 0.5 and 2 keV Ar^+ ions. The silicon concentration during 0.5 keV ion sputtering increases more with temperature than that for 2 keV sputtering. Because the 2 keV ion sputtering rate is higher than the 0.5 keV ion sputtering rate, the silicon atoms that segregate to the surface at higher temperatures are removed faster by the 2 keV ions than by the 0.5 keV ions.

After equilibrium was reached at E and F in Fig. 5, the sample was cooled down to room temperature. As for the other samples, oxygen was then introduced into the vacuum system and Auger peakshapes were measured. Fig. 3d shows the development of the peaks

at the indicated oxygen exposures. By comparing these peaks to the other curves in Fig. 3 it can be inferred that the rate of oxidation is even more reduced for the silicon rich sample. This is also in agreement with the uptake curves shown in Fig. 4.

4. Conclusions

The concentration of the FeSi surface depends on the energy at which it was sputtered. It was shown that the concentration of the altered layer, that was formed during bombardment with higher energy Ar⁺ ions, can be obtained by sputtering with low-energy (0.5 keV) Ar⁺ ions. The oxidation rate of FeSi increases, although not significantly, with decreasing the ion energy at which the sample was sputtered before oxidation. This may be due to the difference in silicon concentration. It was also shown that the segregation rate of silicon during annealing of FeSi depends on the ion energy at which it was sputtered clean. After annealing the FeSi at 593 K and cooling it to room temperature, the oxidation rate decreases further. This work has shown the need for being careful in interpreting results in surface analysis wherever ion beams are used. When the sample that is investigated contains a high concentration of the segregation species, the effect of the ion beam on the surface and the near surface concentration must be kept in mind.

Acknowledgements

The financial support of the University of the Orange Free State and the Foundation for Research and Development are gratefully acknowledged.

References

1. M. BARTUR, *Thin Solid Films* **107** (1983) 55.
2. A. CROS, R. A. POLLAK and K. N. TU, *ibid.* **104** (1983) 221.
3. S. VALERIE, U. del PENNINO and P. SASSAROLI, *Surface Sci.* **134** (1983) L537.
4. M. CLEMENT, J. M. SANZ and J. M. MARTINEZ-DUART, *Surf. Interface Anal.* **15** (1990) 440.
5. G. R. CASTRO and A. BALLESTEROS, *Surface Sci.* **204** (1988) 415.
6. R. SMITH and J. M. WALLS, "Methods of surface analysis", 1st Edn (Cambridge University Press, New York, 1989).
7. A. VAN OOSTROM, *J. Vac. Sci. Technol.* **13** (1976) 224.
8. D. BRIGGS and M. P. SEAH, "Practical Surface Analysis by Auger and X-ray Photoelectron Spectroscopy" (Wiley, New York, 1983).
9. R. SHIMIZU, *Jpn J. Appl. Phys.* **22** (1983) 1631.
10. A. JOSHI, L. E. DAVIS and P. W. PALMBERG, in "Methods of Surface Analysis", edited by A. W. Czanderna (Elsevier Scientific, New York 1975).
11. R. KELLY and A. OLIVA, in "Erosion and growth of solids stimulated by atom and ion beams", edited by G. Kiriakidis *et al.* (Nijhoff, Dordrecht, 1986) p. 41.
12. R. KELLY, *Nucl. Instrum. Meth. Phys. Res.* **B39** (1989) 43.
13. P. H. HOLLOWAY and R. S. BHATTACHARYA, *J. Vac. Sci. Technol.* **20** (1982) 444.
14. J. F. ZIEGLER, J. P. BIRSACK and G. CUOMO, "Stopping and range of ions in matter" (TRIM-88).
15. J. P. BIRSACK and L. G. HAGGMARK, *Nucl. Instrum. Meth.* **174** (1980) 257.
16. B. CARRIERE and J. P. DEVILLE, *Surface Sci.* **80** (1979) 278.
17. M. G. RAMSEY and G. J. RUSSELL, *Phys. Rev. B* **30** (1984) 6960.
18. L. E. DAVIES, N. C. McDONALD, P. W. PALMBERG, G. E. RIACH and R. E. WEBER, "Handbook of Auger Electron Spectroscopy", 2nd Edn (Physical Electronics Division, USA, Minnesota 1978).

*Received 12 November 1991
and accepted 11 August 1992*